Interface-induced anomalous Nernst effect in Fe₃O₄/Pt-based heterostructures

R. Ramos,[1,a)] T. Kikkawa,[1,2] A. Anadón,[3] I. Lucas,[4,5,6] T. Niizeki,[1] K. Uchida,[2,7,8] P. A. Algarabel,[5,9] L. Morellón,[4,5,6] M. H. Aguirre,[4,5,6,10] M. R. Ibarra,[4,5,6,10] and E. Saitoh[1,2,8,11,12]

AFFILIATIONS

[1]Advanced Institute for Materials Research, Tohoku University, Sendai 980-8577, Japan
[2]Institute for Materials Research, Tohoku University, Sendai 980-8577, Japan
[3]IMDEA Nanociencia, Campus de Cantoblanco, 28049 Madrid, Spain
[4]Instituto de Nanociencia de Aragón, Universidad de Zaragoza, E-50018 Zaragoza, Spain
[5]Departamento de Física de la Materia Condensada, Universidad de Zaragoza, E-50009 Zaragoza, Spain
[6]Fundación Instituto de Nanociencia de Aragón, E-50018 Zaragoza, Spain
[7]National Institute for Materials Science, Tsukuba 305-0047, Japan
[8]Center for Spintronics Research Network, Tohoku University, Sendai 980-8577, Japan
[9]Instituto de Ciencia de Materiales de Aragón, Universidad de Zaragoza and Consejo Superior de Investigaciones Científicas, 50009 Zaragoza, Spain
[10]Laboratorio de Microscopías Avanzadas, Universidad de Zaragoza, E-50018 Zaragoza, Spain
[11]Department of Applied Physics, The University of Tokyo, Tokyo 113-8656, Japan
[12]Advanced Science Research Center, Japan Atomic Energy Agency, Tokai 319-1195, Japan

a)ramosr@imr.tohoku.ac.jp

ABSTRACT

We have studied the anomalous Nernst effect (ANE) in [Fe₃O₄/Pt]-based heterostructures grown at high temperature, by measuring the ANE-induced electric field with a magnetic field applied normal to the sample surface, in the perpendicular magnetized configuration, where only the ANEs from the ferromagnetic layers or magnetic proximity effects can be detected. An ANE voltage is observed for [Fe₃O₄/Pt]$_n$ multilayers, and we further investigated its origin by performing measurements in [Fe₃O₄/Pt/Fe₃O₄] trilayers as a function of the Pt thickness. Our results suggest the presence of an interface-induced ANE in the metallic layer, possibly driven by a heat induced subnanometer interdiffusion which affects the nature of the Fe₃O₄/Pt interface. Despite this ANE, the spin Seebeck effect is the dominant mechanism for the transverse thermoelectric voltage in the in-plane magnetized configuration, accounting for about 70% of the voltage in the multilayers.

Published under license by AIP Publishing. https://doi.org/10.1063/1.5063553

Thermoelectricity deals with the study of heat-to-electricity interconversion processes, having the potential for the development of waste heat energy-harvesting technologies. Since the discovery of the spin Seebeck effect (SSE),[1,2] a new heat-to-electricity conversion paradigm in magnetic systems was established and has been extensively studied in a wide range of materials.[3,4] This invigorated the field of spin caloritronics,[5,6] which studies the interaction between heat, electron, and spin currents. In the SSE, a spin current[7] is generally created in a ferromagnetic material (F) upon application of a temperature gradient and electrically detected in an adjacent normal metal (N) by the inverse spin Hall effect (ISHE).[8]

The presence of the SSE in magnetic insulators[2] has potential advantages over conventional thermoelectrics due to lower heat dissipation losses. Its experimental geometry, with the thermal and electric current paths perpendicular to each other, is also advantageous for the implementation of thin films and flexible thermoelectric devices.[9,10] However, the low magnitude of the measured voltage is an obstacle for the development of potential SSE applications. In this regard, different possibilities are currently being explored,[4] such as increasing the spin current detection efficiency,[11,12] spin Hall thermopiles,[13] [F/N]$_n$ multilayers,[14−22] or bulk composite systems.[23]

The ISHE-induced electric field, driven by the thermally generated spin currents in the SSE, can be written as

$$\mathbf{E}_{ISHE} = \theta_{SH}\rho(\mathbf{J}_S \times \boldsymbol{\sigma}), \quad (1)$$

where θ_{SH} and ρ denote the spin Hall angle and electric resistivity of N, respectively. $\mathbf{E}_{ISHE}$, $\mathbf{J}_S$, and $\boldsymbol{\sigma}$ are the ISHE generated electric field, spatial direction of spin current (perpendicular to the F/N interface), and spin-polarization vector (parallel to the magnetization, $\mathbf{M}$). The geometry for the detection of the ISHE is similar to that of the ANE in electrically conductive ferromagnets, which is described by the following expression:[24]

$$\mathbf{E}_{ANE} = Q_S\mu_0(\nabla T \times \mathbf{M}), \quad (2)$$

where Q_S, μ_0, ∇T, and $\mathbf{E}_{ANE}$ are the ANE coefficient, vacuum permeability, applied thermal gradient, and ANE-induced electric field, respectively. Therefore, when using ferromagnetic metals, care must be taken in order to separate the contribution of the SSE from that of the ANE.[25,26] In the case of Fe_3O_4/Pt, the ANE contribution from Fe_3O_4 is expected to be negligibly small due to the resistivity of Fe_3O_4 being two orders of magnitude larger than that of Pt.[27]

Another source of the ANE-driven electric field can be due to a possible magnetic proximity effect (MPE) at the Fe_3O_4/Pt interface. In the case of YIG/Pt and other insulating ferrimagnetic oxides, studies based on x-ray techniques [X-ray magnetic circular dichroism (XMCD) and X-ray resonant magnetic reflectivity (XRMR)] have shown a negligible small MPE;[28–31] in contrast, Lu et al.[32] have reported a non-negligible MPE on a magnetic insulator/Pt system although the reason for this discrepancy is not clear. Recently, XMCD measurements in a Fe_3O_4/Pt/Fe_3O_4 trilayer grown at high temperature[33] have shown a large induced magnetic moment in the Pt interlayer, and therefore, investigating its effect on the thermally driven magnetotransport properties[26] is important to gain further insight into the heat-to-electricity conversion process in [Fe_3O_4/Pt]-based heterostructures. To this purpose, we have performed measurements of the longitudinal SSE,[34] with an in-plane magnetic field (IM) [Fig. 1(a)], and the ANE with a magnetic field applied perpendicular to the sample surface (PM) [Fig. 1(c)]. The measurements in the PM configuration provide a direct measurement of the ANE in the F/N heterostructures due to the fact that, in this configuration, any injected spin current is parallel to the direction of the magnetic field $\mathbf{H}$ ($\mathbf{J}_S \parallel \mathbf{H} \parallel z$) and $E_{ISHE} = 0$ due to the ISHE geometry [Eq. (1)].[3,35]

Here, we have studied two types of Fe_3O_4/Pt-based heterostructures: [Fe_3O_4/Pt]$_n$ multilayers (these are the same samples used in our previous studies)[14–16,20,21] and [Fe_3O_4/Pt(t_{Pt})/Fe_3O_4] trilayers with nominal Pt thicknesses ranging from 1 to 40 nm. The Fe_3O_4 films were grown on MgO(001) substrates by pulsed laser deposition in an ultrahigh-vacuum chamber (UHV). The Pt films were sequentially deposited by DC magnetron sputtering in the same UHV chamber. The substrate temperature during the entire thin film growth process was kept at 480 °C. The structural quality of the samples was confirmed by x-ray diffraction and high angle annular dark field (HAADF) scanning transmission electron microscopy (STEM); detailed information about sample preparation and characterization can be found elsewhere.[14] For the thermoelectric measurements, we employ the temperature difference (ΔT) method[34,36] (supplementary material) and a constant heat power is applied to sustain a similar ΔT for all the samples in each configuration and to minimise thermal
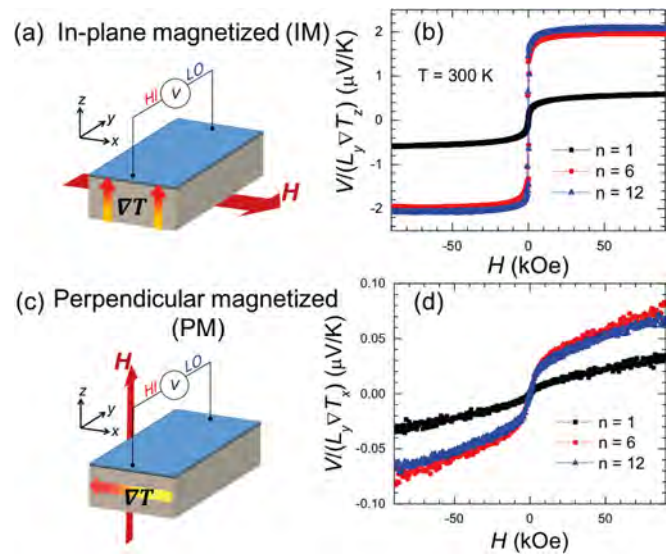

FIG. 1. (a) and (c) Schematic illustrations of the (a) IM and (c) PM configurations conventionally used for the measurement of the (a) longitudinal SSE in magnetic insulators and (c) ANEs. (b) Thermoelectric voltage (SSE + ANE) measured in [Fe_3O_4(23)/Pt(7)]$_n$ (thickness in nm) multilayers in the IM configuration. (d) Thermoelectric voltage (ANE) measured in the PM configuration for [Fe_3O_4(23)/Pt(7)]$_n$ multilayers.

contact resistance errors; other possibility to avoid these is the heat flux method;[37–39] however, it is more sensitive to heat leakages.

Figures 1(b) and 1(d) show the results of the transverse thermoelectric voltage for the [Fe_3O_4/Pt]$_n$ multilayers in the IM [Fig. 1(a)] and PM [Fig. 1(c)] configurations, respectively. The voltage measured in the IM configuration is more than one order of magnitude larger than that observed in the PM configuration. However, to quantitatively compare these voltages, we need to know the temperature gradient distribution in the sample. In the PM configuration, both the multilayer and the substrate are subjected to the same thermal gradient since they are in direct contact with the heat conducting AlN plates (see supplementary material). However, in the IM configuration, we need to evaluate the thermal gradient distribution across the thickness direction ($\parallel z$). By considering heat conservation across the direction of applied heat current, we can estimate that the ANE in the [Fe_3O_4/Pt]$_n$ multilayers accounts for about 30% of the measured voltage in the IM configuration (supplementary material), indicating that there is a non-negligible contribution from the spin-polarized conduction electrons to the transverse thermoelectric voltage, although smaller than the SSE voltage.

In order to gain further insight into the nature of the ANE contribution, we systematically measured the transverse thermoelectric voltage in [Fe_3O_4/Pt(t_{Pt})/Fe_3O_4] trilayers with different platinum thicknesses, t_{Pt}. Figures 2(a) and 2(b) show the voltages measured in the IM and PM configurations, respectively. As shown in the inset of Fig. 2(a), the voltage in the IM configuration continuously increases as the Pt thickness decreases with a maximum at 3 nm and then rapidly decreases, in agreement with that previously reported in a YIG/Pt system.[40] In contrast, the ANE-induced thermoelectric voltage in the PM configuration shows a monotonic increase in the magnitude as the Pt thickness decreases [inset of Fig. 2(b)].
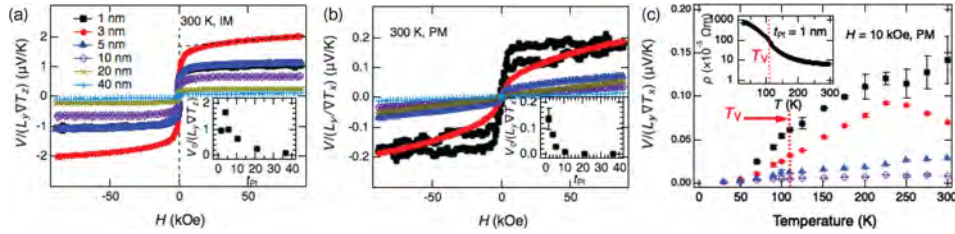
FIG. 2. (a) and (b) Magnetic field dependence of the transverse thermoelectric voltage measured in the (a) IM and (b) PM configurations for [Fe$_3$O$_4$(50)/Pt(t_{Pt})/Fe$_3$O$_4$(50)] tri-layers with different nominal Pt thicknesses. The insets of (a) and (b) show the magnitude of the intercept at zero field of the measured voltage [$V_0/(L_y \nabla T_{(z,x)})$], determined by linear extrapolation of the high field data as schematically depicted by the dashed line of (a). (c) Temperature dependence of the magnitude of the transverse thermoelectric voltage in the PM configuration at $H = 10$ kOe for t_{Pt} between 1 and 10 nm, obtained from the measured magnetic field dependence of the voltage at each temperature. The inset shows the temperature dependence of the resistivity of a Fe$_3$O$_4$/Pt(1)/Fe$_3$O$_4$ trilayer, showing that for this t_{Pt} value, the Fe$_3$O$_4$ layer dominates the transport properties.

The observed ANE can originate from the ANE of Fe$_3$O$_4$[24] or the presence of a magnetic interlayer at the Fe$_3$O$_4$/Pt interface. Under the first scenario, the observed ANE voltage is expected to be strongly suppressed below the metal-insulator transition [Verwey transition, T_V ~110 K for these films, see the inset of Fig. 2(c)]. This is due to the even larger resistivity of Fe$_3$O$_4$ and the increased shunting effect by the Pt layer. However, the temperature dependence of the thermoelectric voltage in the PM configuration [Fig. 2(c)] shows a non-negligible voltage even at temperatures lower than T_V, suggesting that the ANE signal might be originated in the metallic layer at the Fe$_3$O$_4$/Pt interface.

Let us now focus on the thickness dependence of the ANE voltage measured in the PM configuration at room temperature. To analyze the result, we consider an equivalent circuit model in which a magnetic interlayer of thickness t_{MP} is included at the Fe$_3$O$_4$/Pt interfaces [Fig. 3(a)]. This model describes the two previous scenarios where the ANE can originate from the Fe$_3$O$_4$ film (E_F) and in the interface region (E_{MP}). The resultant electric field in the non-magnetic Pt layer (E_y) is expressed as

$$E_y = \frac{1}{1 + \frac{\rho_F \rho_{MP}(t_{Pt} - 2t_{MP})}{2\rho_{Pt}(t_F\rho_{MP} + t_{MP}\rho_F)}} \left[\frac{t_F\rho_{MP}E_F + t_{MP}\rho_F E_{MP}}{t_F\rho_{MP} + t_{MP}\rho_F} \right], \quad (3)$$

where ρ_F (ρ_{MP}, ρ_{Pt}) and t_F (t_{MP}, t_{Pt}) represent the resistivity and the thickness of the Fe$_3$O$_4$ (MPE, Pt) layer, respectively. We consider $\rho_F = 6.96 \times 10^{-5}$ Ωm[14] and $\rho_{MP} = \rho_{Pt}$ (since they represent the magnetic and non-magnetic parts of the Pt layer). The thickness dependence of the Pt resistivity in the trilayers with $t_{Pt} > 3$ nm [Fig. 3(b)] is well described by conventional electron transport in metals,[41,42] and this needs to be considered (supplementary material) to include the thickness dependence of the ANE into our model [Eq. (3)]. In Eq. (3), all the parameters are known, except for E_{MP} and t_{MP}. We can estimate the value of E_{MP} using the model proposed by Guo et al.,[43] where they theoretically estimated the ANE in a magnetized Pt as a function of the induced spin magnetic moment (m_S). With their estimation and the value of $m_S = 0.34 \pm 0.04$ μ_B for Pt recently measured by XMCD in a Fe$_3$O$_4$/Pt(~2 nm)/Fe$_3$O$_4$ trilayer by Kikkawa et al.,[33] we obtain the induced ANE electric field as a function of the Pt resistivity ($E_{MP}/\nabla T = 2.5 \rho_{Pt}$, where the resistivity prefactor unit is Am^{-1} K^{-1}).

Now, we can analyze the thickness dependence of the ANE using Eq. (3). First, we evaluate the ANE of only the Fe$_3$O$_4$ layers, described by considering $t_{MP} = 0$ nm as shown in Fig. 3(d); the magnitude of E_y

thus obtained cannot explain our results, with a lower magnitude of the ANE. If we now introduce a non-negligible t_{MP}, we can reproduce the results with a value of the magnetic Pt thickness of about $t_{MP} = 0.1$ nm; this is significantly smaller than that obtained from XMCD and XRMR studies of Fe/Pt layers,[29,44,45] which might possibly suggest an overestimation of the E_{MP} value. The thickness t_{MP} is also smaller than a possible interdiffusion region at the Fe$_3$O$_4$/Pt interface, as suggested by STEM elemental mapping measured by electron energy loss (EELS) and electron dispersive x-ray (EDX) spectroscopies in a [Fe$_3$O$_4$/Pt/Fe$_3$O$_4$] trilayer with $t_{Pt} = 10$ nm [Fig. 3(c)], which suggest a small interface region of about 0.5 nm, where the Fe and Pt signals overlap. Even after considering a possible magnetic interdiffusion layer into our model, a non-negligible t_{MP} is needed to explain the results
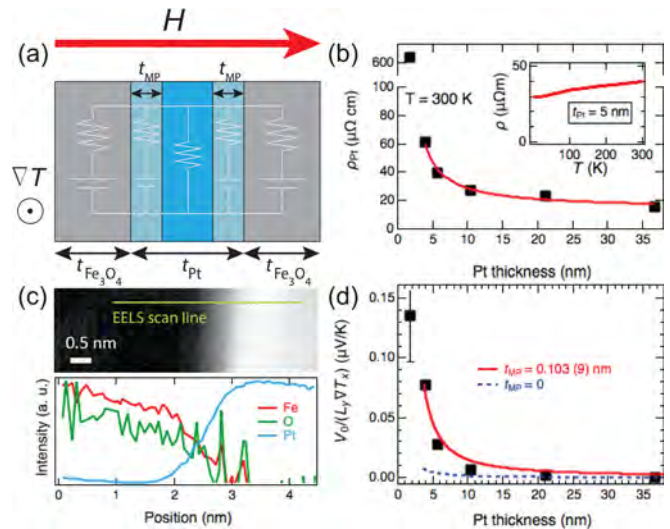
FIG. 3. (a) Schematic diagram of the model used to include a magnetic layer region between the non-magnetic Pt and the Fe$_3$O$_4$ layer. (b) Thickness dependence of the Pt resistivity and fit using the conventional transport formula for metals [the Pt thickness (t_{Pt}) measured by X-ray reflectivity is shown]. (c) STEM image of the Fe$_3$O$_4$/Pt interface of a [Fe$_3$O$_4$(50)/Pt(10)/Fe$_3$O$_4$(50)] trilayer (top) and elemental maps measured by EELS (Fe and O) and EDX (Pt) at the interface in the region indicated by the scan line (bottom).[33] (d) Thickness dependence of the ANE in the trilayers and fit (red line) of the experimental data using Eq. (3) in the range of Pt thicknesses from 3 to 40 nm (the blue dashed line shows the electric field due to ANE of the Fe$_3$O$_4$ layer only, $t_{MP} = 0$).
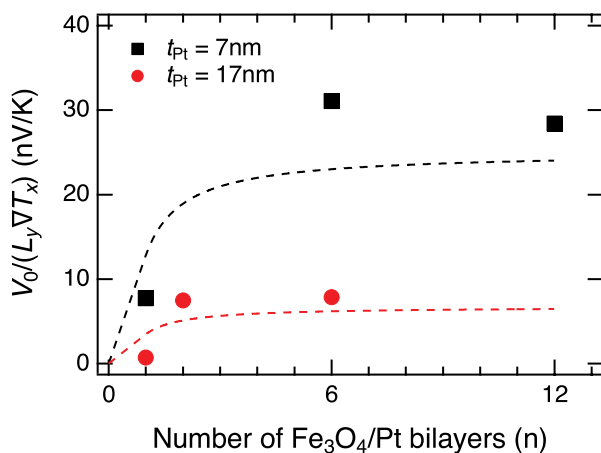
(t_{MP} = 0.06 to 0.1 nm, supplementary material). One possible scenario is that a subnanometer interdiffusion of Fe due to heating induces a modification of the Fe coordination and increases the Fe concentration at the interface.[46,47] This can result in an extrinsically induced Pt magnetic moment around Fe due to a modification of the nature of the F/N interface. This scenario is in agreement with a recent report,[48] further supported by ANE measurements of a Fe₃O₄/Pt bilayer, with Pt films deposited at two different temperatures (room temperature and 480 °C, supplementary material), showing an increase in the ANE for Pt grown at higher temperature and could also possibly explain the non-zero ANE observed for $T < T_V$ [Fig. 2(c)].

Finally, we would like to expand our model to describe the dependence of the interface-induced ANE on the number of multilayers. For a $[Fe_3O_4/Pt]_n$ multilayer, the expression of the ANE-induced electric field is

$$E_y = \frac{1}{1 + \dfrac{\rho_{MP}\rho_F[nt_{Pt} - (2n-1)t_{MP}]}{\rho_{Pt}[nt_F\rho_{MP} + (2n-1)t_{MP}\rho_F]}} \times \left[\frac{nt_F\rho_{MP}E_F + (2n-1)t_{MP}\rho_F E_{MP}}{nt_F\rho_{MP} + (2n-1)t_{MP}\rho_F}\right]. \quad (4)$$

Using the values of E_{MP} and t_{MP} previously estimated, we can obtain the dependence of the interface-induced ANE as a function of the number of layers n. Figure 4 shows the comparison between the ANE measured in the PM configuration for two sets of multilayers with t_{Pt} = 7 and 17 nm and the estimation using Eq. (4). Our model can describe the dependence of the ANE-induced electric field with the number of bilayers (n) and the layer thicknesses, and the magnitude of the predicted ANE in the multilayers is slightly smaller than the measured one especially in the case of thinner samples. The observed magnitude difference could be possibly due to the presence of additional contributions, such as interface-roughness-induced spin-orbit effects in the ferromagnetic layer,[49] which can generate ANE-like voltages as suggested in Ref. 18.

In summary, we observed a non-negligible ANE in $[Fe_3O_4/Pt]_n$ multilayers and investigated its origin by systematic measurements in $[Fe_3O_4/Pt/Fe_3O_4]$ trilayers as a function of the Pt thickness. The results can be understood by an interface-induced ANE, with its origin possibly due to a heat-induced subnanometer Fe-Pt interdiffusion, which possibly affects the Fe coordination and/or the elemental composition at the interface. Measurements of the magnetic moment and length-scale of the magnetic interface (t_{MP}) as a function of Pt deposition temperature obtained by other techniques (XMCD and XRMR) can help to further clarify the origin of the observed effect. These results suggest the possibility of tuning the thermoelectric response by thermal treatment and that, although the SSE is the dominant mechanism, the interface-induced ANE can positively contribute to the spin-induced thermopower in multilayer systems.

See supplementary material for the details of thermoelectric measurements, comparison between IM and PM configurations, Pt resistivity, analysis using a magnetic interdiffusion layer, and effect of Pt deposition temperature.

FIG. 4. Magnitude of the ANE obtained from the zero field intercept in the PM configuration for $[Fe_3O_4(23)/Pt(7)]_n$ (black squares) and $[Fe_3O_4(34)/Pt(17)]_n$ (red circles) multilayers. The dashed lines show the ANE contribution estimated using Eq. (4), considering t_{MP} = 0.1 nm.

REFERENCES

[1] K. Uchida, S. Takahashi, K. Harii, J. Ieda, W. Koshibae, K. Ando, S. Maekawa, and E. Saitoh, Nature **455**, 778 (2008).

[2] K. Uchida, J. Xiao, H. Adachi, J. Ohe, S. Takahashi, J. Ieda, T. Ota, Y. Kajiwara, H. Umezawa, H. Kawai et al., Nat. Mater. **9**, 894 (2010).

[3] K. Uchida, M. Ishida, T. Kikkawa, A. Kirihara, T. Murakami, and E. Saitoh, J. Phys.: Condens. Matter **26**, 343202 (2014).

[4] K. Uchida, H. Adachi, T. Kikkawa, A. Kirihara, M. Ishida, S. Yorozu, S. Maekawa, and E. Saitoh, Proc. IEEE **104**, 1946 (2016).

[5] G. E. W. Bauer, E. Saitoh, and B. J. van Wees, Nat. Mater. **11**, 391 (2012).

[6] S. R. Boona, R. C. Myers, and J. P. Heremans, Energy Environ. Sci. **7**, 885 (2014).

[7] S. Maekawa, H. Adachi, K. Uchida, J. Ieda, and E. Saitoh, J. Phys. Soc. Jpn. **82**, 102002 (2013).

[8] E. Saitoh, M. Ueda, H. Miyajima, and G. Tatara, Appl. Phys. Lett. **88**, 182509 (2006).

[9] A. Kirihara, K. Uchida, Y. Kajiwara, M. Ishida, Y. Nakamura, T. Manako, E. Saitoh, and S. Yorozu, Nat. Mater. **11**, 686 (2012).

[10] A. Kirihara, K. Kondo, M. Ishida, K. Ihara, Y. Iwasaki, A. Matsuba, K. Uchida, E. Saitoh, N. Yamamoto, and T. Murakami, Sci. Rep. **6**, 23114 (2016).

[11] Y. Niimi, Y. Kawanishi, D. H. Wei, C. Deranlot, H. X. Yang, M. Chshiev, T. Valet, A. Fert, and Y. Otani, Phys. Rev. Lett. **109**, 156602 (2012).

[12] Z. Jiang, C.-Z. Chang, M. R. Masir, C. Tang, Y. Xu, J. S. Moodera, A. H. MacDonald, and J. Shi, Nat. Commun. **7**, 11458 (2016).

[13]K. Uchida, T. Nonaka, T. Yoshino, T. Kikkawa, D. Kikuchi, and E. Saitoh, Appl. Phys. Express **5**, 093001 (2012).

[14]R. Ramos, T. Kikkawa, M. H. Aguirre, I. Lucas, A. Anadón, T. Oyake, K. Uchida, H. Adachi, J. Shiomi, P. A. Algarabel, L. Morellón, S. Maekawa, E. Saitoh, and M. R. Ibarra, Phys. Rev. B **92**, 220407(R) (2015).

[15]R. Ramos, A. Anadón, I. Lucas, K. Uchida, P. A. Algarabel, L. Morellón, M. H. Aguirre, E. Saitoh, and M. R. Ibarra, APL Mater. **4**, 104802 (2016).

[16]R. Ramos, T. Kikkawa, A. Anadón, I. Lucas, K. Uchida, P. A. Algarabel, L. Morellón, M. H. Aguirre, E. Saitoh, and M. R. Ibarra, AIP Adv. **7**, 055915 (2017).

[17]K.-D. Lee, D.-J. Kim, H. Yeon Lee, S.-H. Kim, J.-H. Lee, K.-M. Lee, J.-R. Jeong, K.-S. Lee, H.-S. Song, J.-W. Sohn et al., Sci. Rep. **5**, 10249 (2015).

[18]K. Uchida, T. Kikkawa, T. Seki, T. Oyake, J. Shiomi, Z. Qiu, K. Takanashi, and E. Saitoh, Phys. Rev. B **92**, 094414 (2015).

[19]Y. Shiomi, Y. Handa, T. Kikkawa, and E. Saitoh, Appl. Phys. Lett. **106**, 232403 (2015).

[20]K. Uchida, R. Iguchi, S. Daimon, R. Ramos, A. Anadón, I. Lucas, P. A. Algarabel, L. Morellón, M. H. Aguirre, M. R. Ibarra, and E. Saitoh, Phys. Rev. B **95**, 184437 (2017).

[21]R. Ramos, I. Lucas, P. Algarabel, L. Morellón, K. Uchida, E. Saitoh, and M. Ibarra, J. Phys. D: Appl. Phys. **51**, 224003 (2018).

[22]C. Fang, C. H. Wan, Z. H. Yuan, L. Huang, X. Zhang, H. Wu, Q. T. Zhang, and X. F. Han, Phys. Rev. B **93**, 054420 (2016).

[23]S. R. Boona, K. Vandaele, I. N. Boona, D. W. McComb, and J. P. Heremans, Nat. Commun. **7**, 13714 (2016).

[24]R. Ramos, M. H. Aguirre, A. Anadón, J. Blasco, I. Lucas, K. Uchida, P. A. Algarabel, L. Morellón, E. Saitoh, and M. R. Ibarra, Phys. Rev. B **90**, 054422 (2014).

[25]J. Holanda, O. Alves Santos, R. O. Cunha, J. B. S. Mendes, R. L. Rodríguez-Suárez, A. Azevedo, and S. M. Rezende, Phys. Rev. B **95**, 214421 (2017).

[26]P. Bougiatioti, C. Klewe, D. Meier, O. Manos, O. Kuschel, J. Wollschläger, L. Bouchenoire, S. D. Brown, J.-M. Schmalhorst, G. Reiss et al., Phys. Rev. Lett. **119**, 227205 (2017).

[27]R. Ramos, T. Kikkawa, K. Uchida, H. Adachi, I. Lucas, M. H. Aguirre, P. Algarabel, L. Morellón, S. Maekawa, E. Saitoh et al., Appl. Phys. Lett. **102**, 72413 (2013).

[28]S. Geprägs, S. Meyer, S. Altmannshofer, M. Opel, F. Wilhelm, A. Rogalev, R. Gross, and S. T. B. Goennenwein, Appl. Phys. Lett. **101**, 262407 (2012).

[29]T. Kuschel, C. Klewe, J.-M. Schmalhorst, F. Bertram, O. Kuschel, T. Schemme, J. Wollschläger, S. Francoual, J. Strempfer, A. Gupta et al., Phys. Rev. Lett. **115**, 097401 (2015).

[30]M. Valvidares, N. Dix, M. Isasa, K. Ollefs, F. Wilhelm, A. Rogalev, F. Sánchez, E. Pellegrin, A. Bedoya-Pinto, P. Gargiani et al., Phys. Rev. B **93**, 214415 (2016).

[31]M. Collet, R. Mattana, J. Moussy, K. Ollefs, S. Collin, C. Deranlot, A. Anane, V. Cros, F. Petroff, F. Wilhelm et al., Appl. Phys. Lett. **111**, 202401 (2017).

[32]Y. M. Lu, Y. Choi, C. M. Ortega, X. M. Cheng, J. W. Cai, S. Y. Huang, L. Sun, and C. L. Chien, Phys. Rev. Lett. **110**, 147207 (2013).

[33]T. Kikkawa, M. Suzuki, R. Ramos, M. H. Aguirre, K. Uchida, I. Lucas, A. Anadón, D. Kikuchi, J. Okabayashi, P. A. Algarabel, L. Morellón, M. R. Ibarra, and E. Saitoh, "Giant Pt ferromagnetism in $Fe_3O_4/Pt/Fe_3O_4$ epitaxial trilayer detected via X-ray magnetic circular dichroism" (unpublished).

[34]K. Uchida, H. Adachi, T. Ota, H. Nakayama, S. Maekawa, and E. Saitoh, Appl. Phys. Lett. **97**, 172505 (2010).

[35]T. Kikkawa, K. Uchida, Y. Shiomi, Z. Qiu, D. Hou, D. Tian, H. Nakayama, X.-F. Jin, and E. Saitoh, Phys. Rev. Lett. **110**, 067207 (2013).

[36]R. Iguchi, K. Uchida, S. Daimon, and E. Saitoh, Phys. Rev. B **95**, 174401 (2017).

[37]A. Sola, M. Kuepferling, V. Basso, M. Pasquale, T. Kikkawa, K. Uchida, and E. Saitoh, J. Appl. Phys. **117**, 17C510 (2015).

[38]A. Sola, P. Bougiatioti, M. Kuepferling, D. Meier, G. Reiss, M. Pasquale, T. Kuschel, and V. Basso, Sci. Rep. **7**, 46752 (2017).

[39]A. Prakash, B. Flebus, J. Brangham, F. Yang, Y. Tserkovnyak, and J. P. Heremans, Phys. Rev. B **97**, 020408 (2018).

[40]Y. Saiga, K. Mizunuma, Y. Kono, J. C. Ryu, H. Ono, M. Kohda, and E. Okuno, Appl. Phys. Express **7**, 093001 (2014).

[41]K. Fuchs, Math. Proc. Cambridge Philos. Soc. **34**, 100 (1938).

[42]E. Sondheimer, Adv. Phys. **1**, 1 (1952).

[43]G. Y. Guo, Q. Niu, and N. Nagaosa, Phys. Rev. B **89**, 214406 (2014).

[44]J. W. J. Antel, M. M. Schwickert, T. Lin, W. L. O'Brien, and G. R. Harp, Phys. Rev. B **60**, 12933 (1999).

[45]C. Klewe, T. Kuschel, J.-M. Schmalhorst, F. Bertram, O. Kuschel, J. Wollschläger, J. Strempfer, M. Meinert, and G. Reiss, Phys. Rev. B **93**, 214440 (2016).

[46]M. G. Willinger, W. Zhang, O. Bondarchuk, S. Shaikhutdinov, H.-J. Freund, and R. Schlgl, Angew. Chem. Int. Ed. **53**, 5998 (2014).

[47]J. Goniakowski, C. Noguera, L. Giordano, and G. Pacchioni, Phys. Rev. B **80**, 125403 (2009).

[48]H. B. Vasili, M. Gamino, J. Ga, F. Sa, M. Valvidares, P. Gargiani, E. Pellegrin, and J. Fontcuberta, ACS Appl. Mater. Interfaces **10**, 12031 (2018).

[49]L. Zhou, V. L. Grigoryan, S. Maekawa, X. Wang, and J. Xiao, Phys. Rev. B **91**, 045407 (2015).